PROFESSOR XIANZHONG ZHANG (Orcid ID : 0000-0001-8591-8301)

Article type : Research Article

Radioiodinated Estradiol Dimer for Estrogen Receptor Targeted Breast Cancer Imaging

Duo Xu[1]; Chenyu Peng[1]; Fei Gao[1]; Zhide Guo[1]; Rongqiang Zhuang[1]; Xinhui Su[2]; Xianzhong Zhang[1]*

[1] *State Key Laboratory of Molecular Vaccinology and Molecular Diagnostics & Center for Molecular Imaging and Translational Medicine, School of Public Health, Xiamen University, Xiang'an South Rd, Xiamen 361102, China;*

[2] *Zhongshan Hospital Affiliated to Xiamen University, Hubin South Road, Xiamen 361004, China.*

***For correspondence contact:** Xianzhong Zhang, PhD, Professor, Center for Molecular Imaging and Translational Medicine, State Key Laboratory of Molecular Vaccinology and Molecular Diagnostics, School of Public Health, Xiamen University, Xiang'an South Rd., Xiang'an district, Xiamen 361102, China. E-mail: zhangxzh@xmu.edu.cn; Phone: +86(592)2880645; Fax: +86(592)2880645.

First author: Duo Xu, student, Center for Molecular Imaging and Translational Medicine, State Key Laboratory of Molecular Vaccinology and Molecular Diagnostics, School of Public Health, Xiamen University, Xiang'an South Rd., Xiang'an district, Xiamen 361102, China. E-mail: 13164604466@163.com; Phone: +86(592)2880641; Fax: +86(592)2880641.

Author Contributions: The manuscript was written through the contributions of all authors. All authors have given approval to the final version of the manuscript.

Running title: Radioiodinated estradiol dimer for breast cancer imaging

Word count text: 5770 including title page, abstract, and references

This article has been accepted for publication and undergone full peer review but has not been through the copyediting, typesetting, pagination and proofreading process, which may lead to differences between this version and the Version of Record. Please cite this article as doi: 10.1111/CBDD.13754

Abstract

The aim of this study is to develop a 1-(2-(2-(2-(1,2,3-triazol)ethoxy)ethoxy)ethyl)-5-[$^{125/131}$I]iodo-1,2,3-triazole-diestradiol ([$^{125/131}$I]ITE2), for estrogen receptor (ER)-expressing breast cancer imaging with single-photon emission computed tomography (SPECT). [$^{125/131}$I]ITE2 was prepared in good radiochemical yield (94.4 ± 0.4%) with high radiochemical purity (> 99%). [$^{125/131}$I]ITE2 had good stability in vitro and moderate molar activity (0.3 ± 0.2 GBq/μmol). Higher uptake in ER-positive MCF-7 cells than that of ER-negative MDA-MB-231 cells was observed at all time points. Rats biodistribution showed that [^{131}I]ITE2 had high uptake in ER-abundant uterine and ovarian (5.7 ± 0.4 and 10.1 ± 1.4 %ID/g at 1 h post-injection) and could be blocked by co-injection of estradiol (2.7 ± 0.1 and 5.5 ± 0.4 %ID/g) obviously. In the SPECT/CT imaging study, [^{125}I]ITE2 showed significant higher uptake in MCF-7 tumor (3.1 ± 0.4 %ID/g) than that of MDA-MB-231 (0.9 ± 0.1 %ID/g). Furthermore, the specific uptake of [^{125}I]ITE2 in ER-positive MCF-7 tumor could be blocked effectively by pre-administration of fulvestrant (1.2 ± 0.4 %ID/g). A novel radioiodinated dimeric estrogen was designed and synthesized with promising ER targeting ability and specificity. It is worthy of further investigation to validate the advantages of the dimer in ER-positive breast cancer diagnosis.

Key words: radioiodinated dimeric estrogen, estrogen receptor, breast cancer, SPECT/CT imaging, biodistribution.

1. Introduction

The use of estrogen radiopharmaceuticals to image estrogen receptor (ER) in vivo has the potential to determine the ER status of breast cancer. Fluorine-18, iodine-131 and other radionuclides are widely used to label estrogen derivatives for in vivo imaging of ER density in steroid-sensitive tumors (Kiesewetter et al., 1984; Paquette et al., 2013; VanBrocklin et al., 1993; Lim et al. and Mortimer et al., 1996; Xia et al., 2015; Nayak et al., 2008; Neto et al., 2012; Linden et al., 2006; Hochberg, 1979; Ali et al., 1988, 1991, 1993 and 2003; Antunes et al., 2017; Huang et al., 2018; Yan et al., 2013; Rijks et al., 1998; Symes et al., 1985; Gatley et al., 1981). Among them, the most successful ^{18}F-labeled estrogen derivative, 16α-[^{18}F]fluoro-17β-estradiol ([^{18}F]FES), has a good affinity for ER+ tumors and predicts response to tamoxifen (Linden et al., 2006; Mortimer et al., 1996). Meanwhile, a variety of radioiodine-labeled estrogen derivatives for SPECT imaging of ER+ breast cancer have also been reported (Hochberg, 1979; Ali et al., 1988, 1991, 1993 and 2003; Yan et al., 2013; Rijks et al., 1998; Symes et al., 1985). 16α-[^{125}I]iodoestradiol, 11β-methoxy substituent [^{125}I]iodovinylestradiol and its analogs had been reported as potential single photon-emitting ER imaging agents (Hochberg, 1979; Ali et al., 1988, 1991). However, their high thyroid radioactivity uptake suggested severe deiodination occurred in vivo. Just like these probes, metabolic deiodination, resulting in increased non-specific uptake, has become a common problem with radioiodine-labeled-estrogen tracers. Therefore, few radioactive iodine-labeled probes have reached clinical trials so far and recent studies of radioactive iodine-125/131 labeled estrogen ligands are almost stalled while the radioactive fluorine-18 labeled estrogen receptor ligands have been developed rapidly (Antunes et al., 2017; Huang et al., 2018).

From previous research, we know that increasing the metabolic stability is essential for the development of estradiol-skeleton radiotracer. A one-pot, copper(II)-mediated reaction of azides, alkynes, and [^{125}I]iodide to yield 5-[^{125}I]iodo-1,2,3-triazole was reported with high radiochemical yield and good metabolic stability in vivo (Yan et al., 2013). Compared with other multistep radiolabeling methods, the one-step iodo-labeling approach is much easier and more practical for application.

Encouraged by the advantage of the iodo-labeling method and the application of dimers in radiotracer design, the first iodine-125/131 labeled steroidal estrogen dimers, [$^{125/131}$I]ITE2, has been synthesized and labeled in this study. It was prepared by copper-catalyzed reaction of azide, alkyne and iodine to give the metabolically stable 5-iodo-1,2,3-triazole in a single step. In addition, the in vitro and in vivo stabilities, receptor-binding affinity,

biodistribution of the radiotracer were evaluated, and small-animal SPECT/CT imaging of tumor-bearing mice was also performed to verify its feasibility for specific diagnosis of ER-positive breast cancer.

2. Materials and methods

2.1. General

All of the reagents and materials were commercially available. The radioiodine [^{125}I]NaI was bought from China Isotope & Radiation Corporation (Beijing, China) and [^{131}I]NaI was obtained from Zhongshan Hospital Affiliated to Xiamen University. Reversed-phase high-pressure liquid chromatography (HPLC) was performed on a system with an UltiMate 3000 pump (DIONEX) and a B-FC-1000 flow counter (Bioscan). Hypersil GOLD-C18 reversed-phase HPLC column (250*4.6 mm, 5-μm particle size; Thermo Scientific) was used. The mobile phase was changed from 65% of solvent A (water) and 35% solvent B (acetonitrile) to 40% solvent A and 60% solvent B at 10 min. Flow rate: 1 mL/min. Nonradioactive reference [^{127}I]ITE2 was analyzed in the same gradient and monitored at 280 nm. ^{1}H NMR spectra were recorded on a Bruker (400 MHz) spectrometer. Chemical shifts are expressed in ppm (δ) and coupling constants (J) in Hz. Mass spectra were obtained with a Bruker Esquire 3000 plus ESI-MS under electron impact ionization conditions.

All cell lines were purchased from the Type Culture Collection of the Chinese Academy of Sciences (Shanghai, China). The human breast carcinoma MCF-7 cells were cultured in DMEM/high-glucose medium (Gibco, Carlsbad CA, USA) with 10% fetal bovine serum (Gibco), 100 U/mL penicillin, and 100 mg/mL streptomycin (Beyotime, Shanghai, China) in it. The human breast cancer MDA-MB-231 cells were cultured in medium containing 10% fetal bovine serum and 1‰ penicillin/streptomycin. All cells were grown as a monolayer at 37 °C in a moist atmosphere of 5% CO_2 and 95% air.

All procedures and animal use and care protocols were approved by Xiamen University's animal care and use committee (SYXK 2013-0006). The experimental procedures, involving animals, were in accordance with the ethical standards of the institution. The immature female Sprague Dawley rats (3–4 weeks old) and female Balb/c nude mice (18–20 g) were ordered from the Laboratory Animal Center of Xiamen University. MCF-7 cells (2×10^7 cells) or MDA-MB-231 cells (2×10^7 cells) in 100 μL PBS, were injected subcutaneously into the right shoulders of Balb/c nude mice. In vivo SPECT/CT imaging performed when the tumor size reached 0.8–1.2 cm in diameter.

2.2 Chemistry and radiochemistry

The precursor, radioactive [$^{125/131}$I]ITE2 and nonradioactive [^{127}I]ITE2 were synthesized according to the previously reported references (Moldovan et al., 2016; Cao et al., 2017; Ji et al. and Liu et al., 2014; Li et al., 2010). The specific steps are available in scheme 1 and supplementary information. Briefly, the radioiodinated compounds ([^{125}I]ITE2 and [^{131}I]ITE2) were prepared by one-step labeling method and identified by co-injection with the non-radioactive reference compound, their molar activities and radiochemical purities were determined as well using analytical HPLC. After HPLC purification and sterile filtration, the injections were used for the studies of octanol-to-water partition coefficient, stability, receptor-binding and biodistribution ([^{131}I]ITE2) and small-animal SPECT/CT imaging ([^{125}I]ITE2).

2.3 In vivo metabolic stability

The metabolic stability studies in mice were performed in accordance with the published procedures (Mou et al., 2012). Balb/c mice were injected with 7.4 MBq of [^{131}I]ITE2 intravenously and sacrificed at 10, 20, 30 and 60 min post-injection (p.i.). The blood samples were collected and immediately centrifuged at 10,000 rpm for 5 min. After the serum was isolated and added 0.2 mL of methanol, it was centrifuged at 10,000 rpm for 5 min again. The urine samples were collected and centrifuged at 10,000 rpm for 5 min after adding 0.1 mL of methanol. The blood and urine supernatants were collected and passed through a Sep-Pak C18 cartridge (Waters Co., Milford, MA, USA). Then, the cartridges were washed with water (0.5 mL) and eluted with methanol (0.5 mL). The combined aqueous and organic solutions were passed through a 0.22-μm filter (Millipore Co., Billerica, MA, USA) and analyzed by radio-HPLC.

2.4 Receptor-binding studies

Saturation binding assay was performed as described previously (Linden et al., 2006). There were about 2×10^5 MCF-7 cells in each well of a 24-well plate incubated at 37 °C for 24 h. Various concentrations (0–200 nM) of [^{131}I]ITE2 were added and incubated at 37 °C for 1 h. After washing with PBS (1 mL, pH = 7.4) for three times, the cells were lysed with 1 M NaOH (1 mL) for 5-10 min. Radioactivity was measured using a γ-counter (WIZARD 2480, PerkinElmer, USA).

Cell uptakes of [^{131}I]ITE2 in ER-positive MCF-7 and ER-negative MDA-MB-231 cells were studied respectively. After 2×10^5 cells in each well of a 24-well plate were incubated overnight, each well was incubated with [^{131}I]ITE2

(0.185 MBq) at 37 °C for 5, 30, 45, 60, 120, 240 and 360 min. Then, the cells were washed with PBS (1 mL, pH = 7.4) three times and then lysed with 1 M NaOH (1 mL) for 5-10 min. The radioactivity collections were counted using a γ-counter.

To confirm the specificity of the ER binding, MCF-7 cells were treated with ER inhibitor 17β-estradiol (0.17 mM) before incubating with [^{131}I]ITE2 (0.185 MBq) at 37 °C for 5, 30, 45, 60, 120, 240 and 360 min for blocking study. After washing with PBS (1 mL) for three times, the radioactive residues were collected and analyzed using a γ-counter.

2.7 Biodistribution

Biodistribution studies were conducted in accordance with the approved guidelines. The biodistribution of [^{131}I]ITE2 in major organs (n = 3-5/group) was evaluated in immature female SD rats by intravenous injection of 1.85 MBq of [^{131}I]ITE2. Blocking studies were also performed in rats by intravenous co-injection of 1.85 MBq [^{131}I]ITE2 with an excess dose of 17β-estradiol (15 μg/rat). The rats were isoflurane anesthesia, sacrificed and dissected at 1 h or 2 h after injection. Samples of blood, muscle, tumor and major organs were collected and weighted, and then the radioactivity was measured with a γ-counter. The results were expressed as the mean ± SD percentage injected dose per gram (%ID/g).

2.8 Small-animal SPECT/CT imaging

Small-animal SPECT/CT imaging study was performed on ER-positive MCF-7 and ER-negative MDA-MB-231 tumor-bearing nude mice. Each mouse was injected with 18.5 MBq of [^{125}I]ITE2 via the tail vein (n = 3/group). For the blocking study, mice bearing ER+ tumors were subcutaneously injected with the competitive ER-inhibitor fulvestrant (0.5 mg/mouse) at 48 h prior to SPECT/CT imaging. Each mouse was anesthetized and placed on the scanner bed in the prone position. The imaging of [^{125}I]ITE2 was acquired at 15 min or 1 h p.i. and a nanoScan-SPECT/CT preclinical scanner equipped with low energy high-resolution collimators was used. The acquisition parameters: energy peak of 35 keV for ^{125}I, window width of 20%, a matrix of 256 × 256, medium zoom, frame: 30 s. All images were performed in the same manner and reconstructed, processed and further analyzed with Nucline software (Mediso Medical Imaging System) by drawing appropriate Volume of Interests on tumor and muscle.

2.9 Statistical analysis

Differences in data between the experimental, control and inhibition groups were measured by student's t tests and nonparametric tests with the GraphPad prism 5.0 and when *P* is less than 0.05, significant statistical difference is considered between the two groups ($P > 0.05$, $^{*}P < 0.05$, $^{**}P < 0.005$ and $^{***}P < 0.0005$).

3. Results

3.1 Chemistry and radiochemistry

The synthetic routes of [$^{125/131}$I]ITE2 are shown in Scheme 1. [^{125}I]ITE2 was obtained in a radiochemical yield of 94.4 ± 0.4% (n = 5) with a retention time of 10.75 min using radio-HPLC and the radiochemical purity was more than 99% after HPLC purification (Figure 1). The molar activity was 0.3 ± 0.2 GBq/μmol (n = 3) based on the UV standard curve derived from HPLC analysis (Figure S1). The total radiosynthesis time of [^{125}I]ITE2, including HPLC purification, was about 110-120 min. The HPLC retention times of the non-radioactive compound [^{127}I]ITE2 (Figure 1) was 10.65 min. The octanol-to-water partition coefficient (log P) of [^{131}I]ITE2 was calculated as 1.2 ± 0.1, suggesting that it is a lipophilic compound (method was described in the supplementary information). TLC analysis showed that the stability of [^{131}I]ITE2 in physiological saline and murine plasma was maintained for four hours (Figure S2).

3.2 Metabolic stability

[^{131}I]ITE2 found to be metabolic stable in the blood (Figure 2a-b, peak at 10.63 min) at early time points. After 20 min p.i., however, it was metabolized gradually to form a new peak at 3.85 min (Figure 2b-c) and finally the tracer and its metabolite were cleared from the blood at 1 h p.i. (Figure 2d). The metabolite of [^{131}I]ITE2 in the urine was found at 30 min p.i. (Figure 2g, 60%). Thereafter, the peak of [^{131}I]ITE2 gradually disappeared and the metabolite peak at 3.28 min was increased and finally became the only peak at 60 min p.i. (Figure 2h). The radioactive metabolites at 3.85 min and 3.28 min have not been identified while the retention time of free radioiodine was about 3.76 min under the same HPLC conditions.

3.3 Receptor-binding studies

The cell-binding result of [^{131}I]ITE2 was shown in Figure 3a. The dissociation constant (K_d) of [^{131}I]ITE2 was calculated as 49.7 ± 7.7 nM (n = 3). The maximal number of binding sites (B_{max}) was 1.27×10^4 sites per cell.

As shown in Figure 3b, [^{131}I]ITE2 had much higher uptake in ER-positive MCF-7 cells (from 17.9 ± 1.9 to 31.4 ± 3.4 %) than that of ER-negative MDA-MB-231 cells (from 1.1 ± 0.1 to 1.4 ± 0.2 %) at every point of time, which

indicating that [^{131}I]ITE2 has strong affinity to ER-positive MCF-7 cells. The specificity of ER binding was demonstrated in Figures 3c and 3d. After blocking with 0.17 mM of estradiol, the MCF-7 cells uptake was decreased significantly to 5.2 ± 0.1% after 1 h incubation (Figure 3c, ***$P < 0.0001$). Furthermore, the non-specific binding of [^{131}I]ITE2 in ER-negative MDA-MB-231 cells was much lower than that of ER-positive MCF-7 cells after 1 h incubation (***$P < 0.0001$).

3.4 Biodistribution

The biodistribution of [^{131}I]ITE2 was studied in normal female SD rats at 1 and 2 h p.i. As shown in Figure 4a and Table S1, [^{131}I]ITE2 displayed marked uptake and retention of radioactivity in uterine (5.7 ± 0.4 %ID/g and 4.8 ± 0.7 %ID/g at 1 h and 2 h p.i., respectively) and ovarian (10.1 ± 1.4 %ID/g and 10.2 ± 1.8 %ID/g at 1 h and 2 h p.i., respectively), organs known to contain high ER concentrations. The uptake of [^{131}I]ITE2 in non-specific organs and tissue, such as the heart, spleen, lung and muscle, was 1.2 ± 0.0, 1.6 ± 0.2, 0.8 ± 0.2 and 1.5 ± 0.4 %ID/g at 1 h p.i., respectively. Low blood uptake was observed of only 0.7 ± 0.2 %ID/g at 1 h p.i. and the amount of radioactivity remained nearly constant until 2 h p.i. The uptake of fat (2.4 ± 0.4 %ID/g) was lower than that in the uterus and ovaries, but higher than the muscle uptake. Organs involved in steroid hormone metabolism and excretion, such as liver, intestine and kidneys, had the uptakes of 1.3 ± 0.2 %ID/g, 2.3 ± 0.5 %ID/g and 1.1 ± 0.2 %ID/g, respectively. There had no significant difference between the uptakes of thyroid and muscle (2.3 ± 0.6 %ID/g and 1.5 ± 0.4 %ID/g, respectively, $P = 0.1$) of [^{131}I]ITE2 indicating negligible deiodination of it in vivo.

The tissue uptake specificity of the [^{131}I]ITE2 is also presented. Uterus and ovarian uptake were inhibited by the presence of an excess estradiol (2.7 ± 0.1 %ID/g and 5.5 ± 0.4 %ID/g, ***$P = 0.0004$ and *$P = 0.007$, respectively). Radioactivity uptake in the non-target tissues, such as heart, spleen, lung muscle and fat, was not affected by the co-injection of unlabeled estradiol. Besides, the uptake of radioactivity in organs involved in steroid hormone metabolism and excretion (liver, intestine and kidneys), usually no statistically significant decrease in uptake of the [^{131}I]ITE2 was found. The ratios of the uterus to blood and uterus to muscle were 9.2 ± 2.4 and 4.2 ± 1.5 at 1 h p.i. respectively, and decreased sharply to 4.1 ± 1.1 and 1.7 ± 0.2. (Figure 4b, c and Table S1, *$P = 0.02$, $P = 0.06$) after blocking.

3.5 Small-animal SPECT/CT imaging

SPECT/CT images of tumor-bearing mice were acquired at 15 min and 1 h (MCF-7 tumor) or 1 h (MDA-MB-231 tumor) after injection of [^{125}I]ITE2 (Figure 5). MCF-7 tumors were visible as early as 15 min p.i. and tumor uptake increased at 1 h p.i., while MDA-MB-231 tumors showed low radioactive accumulation at 1 h p.i. Under blocking conditions with excess ER-inhibitor fulvestrant, MCF-7 tumor uptake of [^{125}I]ITE2 was reduced significantly at 1 h p.i. As shown in Figure 5b and Figure S3, [^{125}I]ITE2 had obviously higher MCF-7 tumor to muscle ratio (T/M = 2.3 ± 0.6) than that of MDA-MB-231 (T/M = 0.6 ± 0.1, $*P = 0.01$). These results confirm the specificity of [^{125}I]ITE2 for ER-positive tumors in vivo. The MCF-7 tumor uptake of [^{125}I]ITE2 was uneven, mainly due to the fact that MCF-7 tumor is a highly heterogeneous tumor (Yang et al., 2017; Babayan et al., 2013).

4. Discussion

An accurate and noninvasive method of assessing ER status, which avoids unnecessary biopsies and allows for a series of clinical evaluations during breast cancer endocrine therapy, is always necessary. Besides, it has been reported that dimeric and polymeric may enhance the receptor binding affinity by the local enrichment of radiotracer thereby increasing the probability of radiotracer binding to a receptor protein (Chen et al., 2004). To our knowledge, [$^{125/131}$I]ITE2 is the first radioactive iodine-labeled estrogen dimer.

[$^{125/131}$I]ITE2 was prepared successfully with high yield (94.4 ± 0.4%) and good labeling efficiency (about 90 min). While for the classical method of iodine-125 labeled estradiol, it requires an overnight radiolabeling reaction with only 25 to 65% yield (Hochberg, 1979). Furthermore, the formation of 5-[$^{125/131}$I]iodo-1,2,3-triazole was reported to be effective in preventing metabolic deiodination in vivo (Ali et al., 1991). However, the molar activity of [$^{125/131}$I]ITE2 (0.3 ± 0.2 GBq/μmol) is not as high as expected (2−3 GBq/μmol, Yan et al., 2013). The reason for the failure to obtain the theoretical molar activity may be related to the concentration of [$^{125/131}$I]NaI. Nevertheless, the iodinated estrogen, made as described, is more than adequate for use in estrogen receptor studies.

A series of modifications have been made to estrogen to enhance the specificity of steroidal radiotracers for targeted tissues in vivo. For example, 2-F, 4-F and 7α-cyano-substituted radioiodine-labeled estradiol have been reported. Their uterus and thyroid uptakes were 0.46 ± 0.06 %ID/g and 57.96 ± 9.47 %ID/g for 2-F-16α-[^{125}I]IE_2; 2.7 ± 0.10 %ID/g and 43.73 ± 5.67 %ID/g for 4-F-16α-[^{125}I]IE_2; 4.72 ± 0.33 %ID/g and 107.92 ± 24.31 %ID/g for 2-F-11β-OMe-16α-[^{125}I]IE_2 (Ali et al., 1993); 6.35 ± 0.52 %ID/g and 252 ± 11.75 %ID/g for

7-Cyano-16α-[^{125}I]iodoestradiol and 12.77 ± 0.61 %ID/g and 118 ± 8.28 %ID/g for 7-Cyano(17α,20E)[^{125}I]iodovinylestradiol (Ali et al., 2003) at 1 h p.i., respectively. [^{131}I]ITE2 developed in this work showed a moderate uterine uptake (5.7 ± 0.4 %ID/g) with good retention and obviously reduced thyroid uptake (2.3 ± 0.6 %ID/g) when compared to the previously reported probes (Ali et al., 1993, 2003; Rijks et al., 1996, 1998), indicating its binding affinity and good metabolic stability. Furthermore, the low non-specific uptake was fulfilled through the PEGylation of estrogen to reducing lipophilicity.

As we all know, the rapid clearance of the radiotracer in the body causes the relatively low uptake of target sites (Mankoff et al., 1997). If the radiotracer can be stable in the circulation for a longer time, it will have a greater chance of enrichment in the tumor. In this study, about 100% of [^{131}I]ITE2 still exists in intact form after 20 min p.i., much better than that of [^{18}F]FES and 4FM[^{18}F]FES, the classic ER imaging agents, which were rapidly metabolized in blood, resulting in less than 20% of intact radiotracer after only 5 min p.i. (Paquette et al., 2013). Since the heartbeat of mice is faster than humans, it can be predicted that [^{131}I]ITE2 may have a longer metabolic time in the human body, which makes it possible for [$^{125/131}$I]ITE2 to become a radiotracer for imaging and even treating ER+ tumors in the future.

Decades ago, the application of the bivalent concept to the estrogen receptor had been studied by several groups. Among them, Shan et al. (2013) deeply studied the ER-binding affinities and cellular activities of nonsteroidal bivalent estrogen ligands. Their findings on the nature of the ligand, the length and nature of the spacer might be useful for further design of radiolabeled bivalent or multivalent steroidal estrogen ligands. Their study had shown that the use of large polar groups such as carboxylic acids, amides or esters as linkers for divalent ligands will greatly reduce the affinity of divalent molecules to receptors. While PEGylation has been proved to be an effective strategy to enhance the affinity with the optimized distance between the divalent ligands (10.8 Å, ~ 2 PEG). Refer to previous studies, herein we developed a radioiodinated dimeric molecule and evaluated it in vitro and in vivo for ER targeting. However, the direct comparison of the ER binding affinity and targeting ability of this dimeric ligand with an appropriate monovalent control compound should be made in the future to further demonstrate the success of dimerization conception. In addition, we will conduct more in-depth research on estradiol dimers or polymers and the linker type and length between targeting motifs in the future, and the content of the comparison will be reflected in the subsequent research.

So far, none of the radiolabeled steroid agents have been commercialized for routine steroid receptor PET/SPECT imaging. This is mainly because the current clinical research on these imaging agents is not enough. Other than to develop more new estrogen receptor imaging agents, there needs more studies to clarify the tumor uptake threshold of breast cancer, which directly affects the clinical judgment of hormone therapy (Fowler et al., 2016; van Kruchten et al., 2013).

5. Conclusion

A novel radioiodinated estrogen dimer [$^{125/131}$I]ITE2 was prepared successfully in high radiochemical yield with a good specific binding affinity to the estrogen receptor. The metabolic time of [^{131}I]ITE2 in blood has been greatly extended with almost no deiodination, which provides a basis for breast cancer typing and guides the clinical treatment programs. The biological function of the dimeric [$^{125/131}$I]ITE2 can also be optimized by changing the length of the PEG chain to adjust the distance between two estrogen molecules.

Acknowledgments

This study was financially supported by the National Key Basic Research Program of China (2014CB744503), the National Natural Science Foundation of China (21976150) and the Major Research plan of the National Natural Science Foundation of China (91959122).

Conflicts of interest

The authors declare no conflict of interest.

References

Ali H., Rousseau J., Ghaffari M. A., & van Lier J. E. (1988). Synthesis, receptor binding, and tissue distribution of (17α, 20E)- and (17α, 20Z)-21-[^{125}I] iodo-19-norpregna-1,3,5(10), 20-tetraene-3, 17-diol. *Journal of Medicinal Chemistry*, 31, 1946-1950. doi: 10.1021/jm00118a013

Ali H., Rousseau J., Paquette B., Dube C., Marko B., & van Lier J. E. (2003). Synthesis and biological properties of 7α-cyano derivatives of the (17α, 20E/Z)-[^{125}I]iodo-vinyl- and 16α-[^{125}I]iodo-estradiols. *Steroids*, 68, 1189-1200. doi: info:doi/10.1016/j.steroids.2003.09.005

Ali, H., Rousseau, J., Gantchev, T. G., & van Lier, J. E. (1993). 2- and 4-fluorinated 16α-[^{125}I]iodoestradiol derivatives: synthesis and effect on estrogen receptor binding and receptor-mediated target tissue uptake. *Journal of Medicinal Chemistry*, 36, 4255-4263. doi: 10.1021/jm00078a016

Ali, H., Rousseau, J., Ghaffari, M. A., & van Lier, J. E. (1991). Synthesis, receptor binding, and tissue distribution of 7α- and 11β-substituted (17α, 20E)- and (17α, 20Z)-21-[^{125}I]iodo-19-norpregna-1,3,5(10),20-tetraene-3,17-diols. *Journal of Medicinal Chemistry*, 34, 854-860. doi: 10.1021/jm00106a054

Antunes I. F., van Waarde A., Dierckx R. A., de Vries E. G., Hospers G. A., de Vries E. F. (2017). Synthesis and evaluation of the estrogen receptor β-selective radioligand 2-^{18}F-fluoro-6-(6-hydroxynaphthalen-2-yl)pyridin-3-ol: comparison with 16α-^{18}F-fluoro-17β-estradiol. *Journal of Nuclear Medicine*, 58, 554-559. doi: 10.2967/jnumed.116.180158

Babayan A., Hannemann J., Spötter J., Müller V., Pantel K., Joosse S. A. (2013). Heterogeneity of estrogen receptor expression in circulating tumor cells from metastatic breast cancer patients. *PLoS One*, 2013, 8, e75038. doi: 10.1371/journal.pone.0075038

Cao J, Liu Y, Zhang L, Du F, Ci Y, Zhang Y, ... Qiao J. P. (2017). Synthesis of novel PEG-modified nitroimidazole derivatives via “hot-click” reaction and their biological evaluation as potential PET imaging agent for tumors. *Journal of Radioanalytical & Nuclear Chemistry*, 312, 263–276. doi: 10.1007/s10967-017-5210-5

Chen X., Liu S., Hou Y., Tohme M., Park R., Bading J. R., Conti P. S. (2004). MicroPET imaging of breast cancer α_V-integrin expression with ^{64}Cu-labeled dimeric RGD peptides. *Molecular Imaging & Biology*, 6, 350-359. doi: 10.1016/j.mibio.2004.06.004

Fowler A. M., Clark A. S., Katzenellenbogen J. A., Linden H. M., Dehdashti F. (2016). Imaging diagnostic and therapeutic targets: steroid receptors in breast cancer. *Journal of Nuclear Medicine*, 57:75S-80S. doi: 10.2967/jnumed.115.157933

Gatley, S. J, Shaughnessy, W. J, Inhorn, & Leiberman. (1981). Studies with 17β (16α-[^{125}I]iodo)-estradiol, an estrogen receptor-binding radiopharmaceutical, in rats bearing mammary tumors. *Journal of Nuclear Medicine*, 22, 459–464. doi: 10.1097/00004728-198112000-00060

Hochberg, R. B. (1979). Iodine-125--labeled estradiol: a gamma-emitting analog of estradiol that binds to the estrogen receptor. *Science*, 205, 1138-1140. doi: 10.1126/science.472733

Huang, H., Li, K., Lv, G., Liu, G., & Lin, J. (2018). One-step ^{18}F-labeling of estradiol derivative for PET imaging of breast cancer. *Contrast Media & Molecular Imaging*, 2018, 1-9. doi: 10.1155/2018/5362329.

Ji, L., Zhou, G. Q., Qian, C., & Chen, X. Z. (2014). Synthesis of 1,2,3-triazoles from azide-derivatised aminocyclitols by catalytic diazo transfer and CuAAC click chemistry. *European Journal of Organic Chemistry*, 17, 3622-3636. doi: 10.1002/ejoc.201301874

Kiesewetter, D. O., Kilbourn, M. R., Landvatter, S. W., Heiman, D. F., Katzenellenbogen, J. A., Welch, M. J. (1984). Preparation of four fluorine-18-labeled estrogens and their selective uptakes in target tissues of immature rats. *Journal of Nuclear Medicine*, 25, 1212-1221.

van Kruchten, M., de Vries, E. G. E., Brown, M., de Vries, E. F. J., Glaudemans, A. W. J. M., Dierckx, R. A. J. O., ... Hospers, G. A. P. (2013). PET imaging of oestrogen receptors in patients with breast cancer. *Lancet Oncology*, 14, e465-e475. doi: 10.1016/S1470-2045(13)70292-4

Li L., Zhang G., Zhu A., Zhang L. (2008). A convenient preparation of 5-iodo-1,4-disubstituted-1,2,3-triazole: multicomponent one-pot reaction of azide and alkyne mediated by CuI-NBS. *Journal of Organic Chemistry*, 73, 3630-3633. doi: 10.1002/chin.200836130

Lim J. L., Zheng L., Berridge M. S., Tewson T. J. The use of 3-methoxymethyl-16β, 17β-epiestriol-O-cyclic sulfone as the precursor in the synthesis of ^{18}F-16α-fluoroestradiol. (1996). *Nuclear Medicine and Biology*, 23, 911-915. doi: 10.1016/S0969-8051(96)00126-6

Linden, H. M., Stekhova, S. A., Link, J. M., Ellis, G. K., Petra, P. H., Peterson, L. M., ... Mankoff, D. A. (2006). Quantitative fluoroestradiol positron emission tomography imaging predicts response to endocrine treatment in breast cancer. *Journal of Clinical Oncology*, 24, 2793-2799. doi: 10.1200/JCO.2005.04.3810

Liu, Z., Pourghiasian, M., Radtke, M. A., Lau, J., Perrin, D. M., Dias, G. M., ... Perrin, D. M. (2014). An organotrifluoroborate for broadly applicable one-step ^{18}F-labeling. *Angewandte Chemie*, 53, 11876-11880. doi: 10.1002/ange.201406258

Mankoff D. A., Tewson T. J., Eary J. F. (1997). Analysis of blood clearance and labeled metabolites for the estrogen receptor tracer [^{18}F]-16α-fluoroestradiol (FES). *Nuclear Medicine and Biology*, 24, 341–348. doi: 10.1016/S0969-8051(97)00002-4

Moldovan, R. P., Teodoro, R., Gao, Y., Deuther-Conrad, W., Kranz, M., Wang, Y., ... Horti, A. G. (2016). Development of a high-affinity PET radioligand for imaging cannabinoid subtype 2 receptor. *Journal of Medicinal Chemistry*, 59, 7840-7855. doi: 10.1021/acs.jmedchem.6b00554.

Mortimer J. E., Dehdashti F., Siegel B. A., Katzenellenbogen J. A., Fracasso P., & Welch M. J. (1996). Positron emission tomography with 2-[^{18}F]Fluoro-2-deoxy-D-glucose and 16α-[^{18}F]fluoro-17β-estradiol in breast cancer: correlation with estrogen receptor status and response to systemic therapy. *Clinical Cancer Research*, 2, 933-939.

Mou T, Zhao Z, Fang W, Peng C, Guo F, Liu B, ... Zhang X. (2012). Synthesis and preliminary evaluation of ^{18}F-labeled pyridaben analogues for myocardial perfusion imaging with PET. *Journal of Nuclear Medicine*, 53, 472-479. doi: 10.2967/jnumed.111.088096

Nayak, T. K., Hathaway, H. J., Ramesh, C., Arterburn, J. B., Dai, D., Sklar, L. A., ... Prossnitz, E. R. (2008). Preclinical development of a neutral, estrogen receptor-targeted, tridentate ^{99m}Tc(I)-estradiol-pyridin-2-yl hydrazine derivative for imaging of breast and endometrial cancers. *Journal of Nuclear Medicine*, 49, 978-986. doi: 10.2967/jnumed.107.048546

Neto, C., Oliveira, M. C., Gano, L., Marques, F., Yasuda, T., Thiemann, T., ... Santos, I. (2012). Novel 7α-alkoxy-17α-(40-halophenylethynyl)estradiols as potential SPECT/PET imaging agents for estrogen receptor expressing tumours: synthesis and binding affinity evaluation. *Steroids*, 77, 1123–1132. doi: 10.1016/j.steroids.2012.05.004

Paquette, M., Phoenix, S., Ouellet, R., Langlois, R., van Lier, J. E., Turcotte, É. E., ... Lecomte, R. (2013). Assessment of the novel estrogen receptor PET tracer 4-fluoro-11β-methoxy-16α-[^{18}F]fluoroestradiol (4FMFES) by PET imaging in a breast cancer murine model. *Molecular Imaging & Biology*, 15, 625-632. doi: 10.1007/s11307-013-0638-7

Rijks, L. J. M., Boer, G. J., Endert, E., de Bruin, K., van den Bos, J. C., van Doremalen, P. A. P. M., ... van Royen, E. A. (1996). The stereoisomers of 17α-[^{123}I]iodovinyloestradiol and its 11beta-methoxy derivative evaluated for their oestrogen receptor binding in human MCF-7 cells and rat uterus, and their distribution in immature rats. *European Journal of Nuclear Medicine*, 23, 295-307. doi: 10.1007/BF00837628

Rijks, L. J. M., van den Bos, J. C., van Doremalen, P. A. P. M., Boer, G. J., de Bruin, K., Doornbos, T., ... van Royen, E. A. (1998). Synthesis, estrogen receptor binding, and tissue distribution of a new iodovinylestradiol derivative 17α,20E)-21-[^{123}I]Iodo-11β-nitrato-19-norpregna-1,3,5(10),20-tetraene-3,17-diol(E-[^{123}I]NIVE). *Nuclear Medicine & Biology*, 25, 411-421. doi.org/10.1016/S0969-8051(97)00223-0

Shan, M., Carlson, K. E., Bujotzek, A., Wellner, A., Gust, R., Weber, M., ... Haag, R. (2013). Nonsteroidal bivalent estrogen ligands: an application of the bivalent concept to the estrogen receptor. *ACS Chemical Biology*, 8, 707-715. doi: 10.1021/cb3006243

Symes E. K., Coulson W. F., Ralphs D. N. (1985). The synthesis of 16 alpha-[^{131}I]iodo-oestradiol and evaluation of its use as a radiotracer for oestrogen receptor positive breast tumors. *Journal of Steroid Biochemistry*, 22, 155-160. doi: 10.1016/0022-4731(85)90107-4

VanBrocklin H. F., Carlson K. E., Katzenellenbogen J. A., Welch M. J. (1993). 16β-([^{18}F]fluoro)estrogens: systematic investigation of a new series of fluorine-18-labeled estrogens as potential imaging agents for estrogen receptor-positive breast tumors. *Journal of Medicinal Chemistry*, 36, 1619–1629. doi: 10.1021/jm00063a012

Xia, X., Feng, H., Li, C., Qin, C., Song, Y., Zhang, Y., & Lan, X. (2015). ^{99m}Tc-labeled estradiol as an estrogen receptor probe: preparation and preclinical evaluation. *Nuclear Medicine & Biology*, 43, 89–96. doi: 10.1016/j.nucmedbio.2015.09.006

Yan, R., Sander, K., Galante, E., Rajkumar, V., Badar, A., Robson, M., ... Årstad, E. (2013). One-pot three-component radiochemical reaction for rapid assembly of ^{125}I-labeled molecular probes. *Journal of the American Chemical Society*, 135, 703-709. doi: 10.1021/ja307926g

Yang, Z., Sun, Y., Xu, X., Zhang, Y., Zhang, J., Xue, J., ... Zhang, Y. (2017). The assessment of estrogen receptor status and its intratumoral heterogeneity in patients with breast cancer by using ^{18}F-fluoroestradiol PET/CT. *Clinical Nuclear Medicine*, 42, 421-427. doi: 10.1097/RLU.0000000000001587

Figure and Legends

Scheme 1. Synthetic routes of radioiodinated compounds [$^{125/131}$I]ITE2 and non-radioactive compound [^{127}I]ITE2.

Figure 1. The HPLC chromatograms of compound [^{127}I]ITE2 and [^{125}I]ITE2. They were analyzed with the same gradient HPLC method. The non-radioactive compound was measured with a UV detector while the radioactive compound was measured radiometrically.

Figure 2. The HPLC chromatograms of haematic radio-metabolites in mice at (**a**) 10 min, (**b**) 20 min, (**c**) 30 min and (**d**) 60 min. The HPLC chromatograms of urinary radio-metabolites in mice at (**e**) 10 min, (**f**) 20 min, (**g**) 30 min and (**h**) 60 min. The haematic and urinary radio-metabolites were detected at 3.85 min, 3.28 min and 3.01 min, and the intact [^{131}I]ITE2 were detected at 10.63 min, 10.61 min and 10.50 min.

Figure 3. Cell saturation binding, uptake, blocking study of [^{131}I]ITE2. (**a**) Representative results of saturation assay using MCF-7 cells. The curve was generated by measuring the radioactivity in MCF-7 cells incubated with increasing concentrations of [^{131}I]ITE2 as indicated. (**b**) Cell uptake of [^{131}I]ITE2 in MCF-7 and MDA-MB-231 cells; Uptake of [^{131}I]ITE2 in MCF-7 cells was blocked in the presence of 0.17 mM of estradiol. (**c**), (**d**) Cell uptake values of [^{131}I]ITE2 at 1 h from **b**. (***$P < 0.0001$). All data were determined from three independent experiments and expressed as the mean ± SD.

Figure 4. (**a**) Tissue distribution of ^{131}I radioactivity (%ID/g) after intravenous injection of [^{131}I]ITE2 into immature female rats for 1 h and 2 h. A group of animals for the 1 h-blocked experiment received 15 μg/rat of unlabeled estradiol (ES), co-injected with [^{131}I]ITE2 (***$P = 0.0004$). (**b**), (**c**) Uterus to blood ratio and uterus to muscle ratio from **a**. (n = 3 - 5, *$P = 0.02$, $P = 0.06$. Data are means ± SD).

Figure 5. (**a**) Representative SPECT/CT images obtained at 15 min and 1 h p.i. of [^{125}I]ITE2 in nude mice bearing MCF-7 tumor, fulvestrant-treated MCF-7 tumor-bearing nude mice and MDA-MB-231 tumor-bearing nude mice; (**b**) Tumor to muscle ratios were derived from SPECT images (means ± SD, n = 3, *P = 0.01). Tumor sites were indicated by circles.

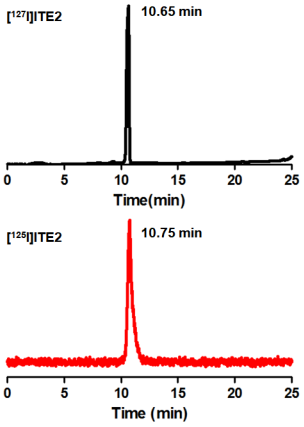

cbdd_13754_f1.png

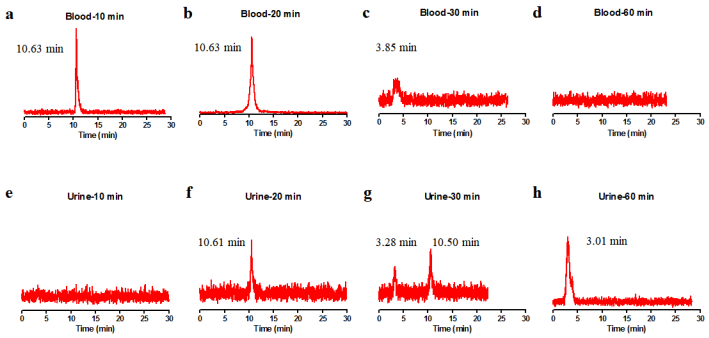

cbdd_13754_f2.png

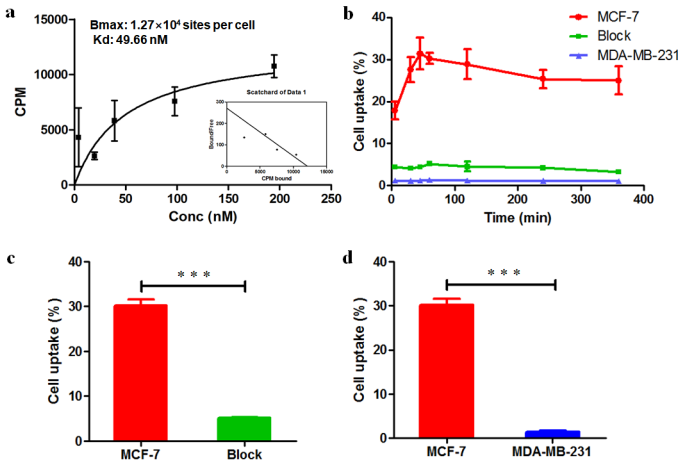

cbdd_13754_f3.png

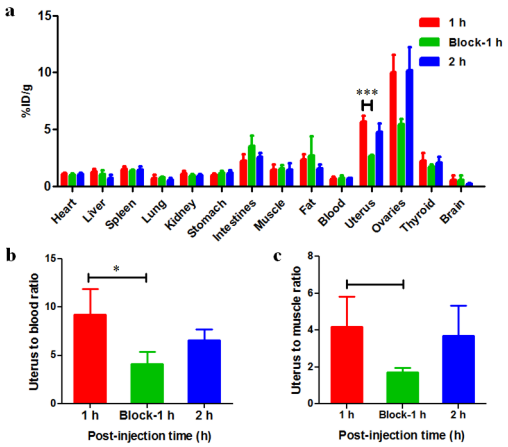

cbdd_13754_f4.png

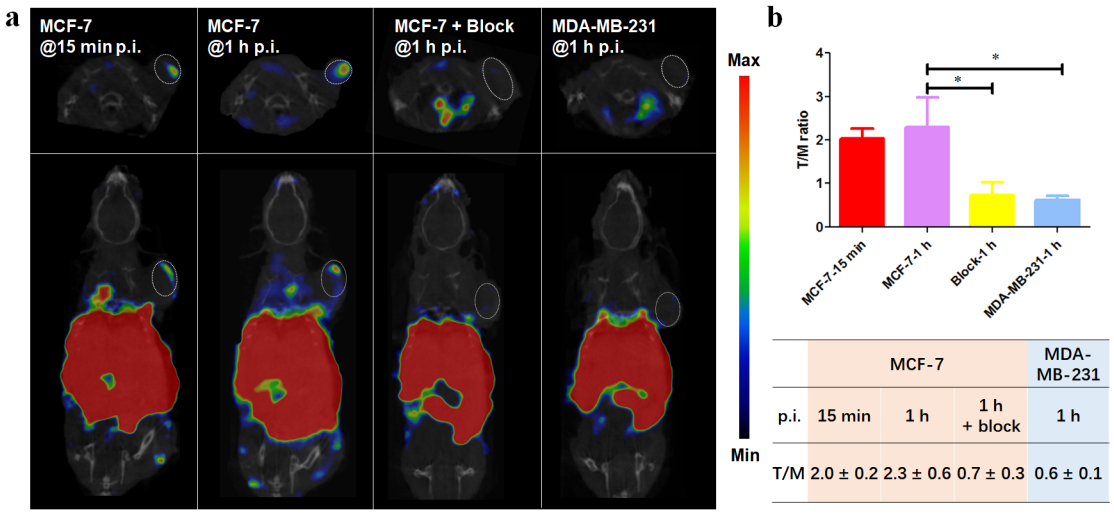

	MCF-7			MDA-MB-231
p.i.	15 min	1 h	1 h + block	1 h
T/M	2.0 ± 0.2	2.3 ± 0.6	0.7 ± 0.3	0.6 ± 0.1

cbdd_13754_f5.png

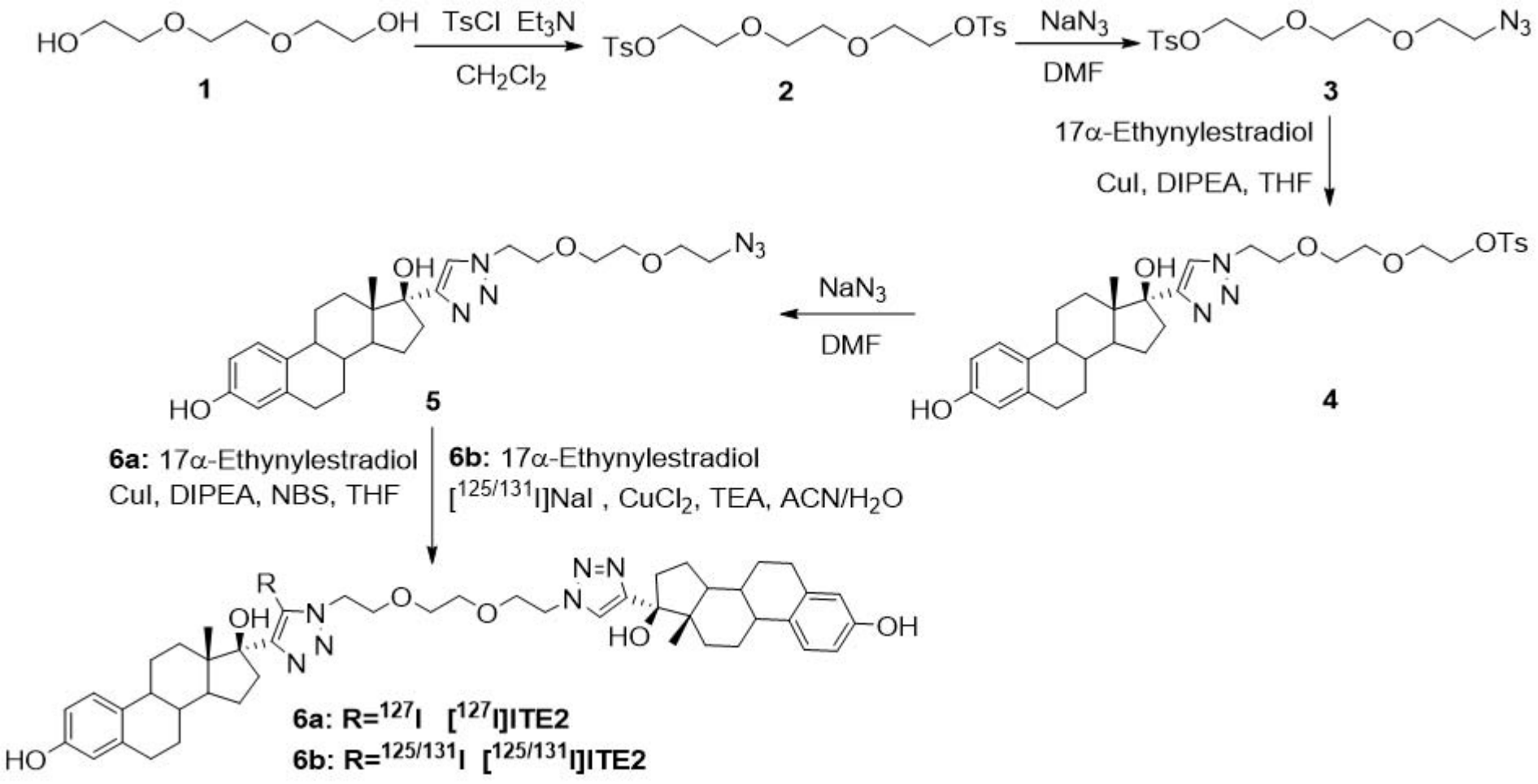
TsCl Et3N
CH2Cl2
NaN3
DMF
17α-Ethynylestradiol
CuI, DIPEA, THF
NaN3
DMF
6a: 17α-Ethynylestradiol
CuI, DIPEA, NBS, THF
6b: 17α-Ethynylestradiol
[125/131I]NaI , CuCl2, TEA, ACN/H2O
1
2
3
4
5
6a: R=127I [127I]ITE2
6b: R=125/131I [125/131I]ITE2